PERGAMON

International Journal of Heat and Mass Transfer 44 (2001) 919–930

International Journal of HEAT and MASS TRANSFER

www.elsevier.com/locate/ijhmt

Fluctuating characteristics and rotation induced stabilization of thermal buoyancy driven water flow in a vertical rotating cylinder

C.P. Yin, Y.T. Ker, T.H. Huang, T.F. Lin *

Department of Mechanical Engineering, National Chiao Tung University, 1001 Ta Hsueh Road, Hsinchu 30049, Taiwan, ROC

Received 15 July 1999; received in revised form 21 April 2000

Abstract

An experimental study was carried out here to investigate the fluctuating characteristics and stabilization of the thermal buoyancy driven unstable water flow in vertical closed circular cylinders heated from below by rotating the cylinder about its vertical axis. Results for the time variations of the water temperature at selected locations were obtained for the imposed temperature difference ΔT ranging from 5°C to 15°C and the cavity rotation rate Ω from 0 to 300 rpm for a cylinder with diameter $D = 5$ cm, height $H = 10$ cm and Ω varying from 0 to 210 rpm for another cylinder with $D = 2.5$ cm and $H = 5$ cm. Based on the data for the time records of the water temperature, the flow suppression by the cylinder rotation causes the time-average temperature distributions along the cylinder axis for high rotation rates to become linear. Besides, the flow can be stabilized by the cylinder rotation when the rotation rate is in certain ranges. Significant dependence of the oscillation amplitude with the space is revealed. But the entire flow oscillates at nearly the same frequency when the flow is time periodic. Moreover, non-monotonic variations of the oscillation frequency with the rotation rate are clearly shown. Based on the present data, a flow regime map and correlations delineating the stable and unstable states in the vertical rotating cylinders containing water are also provided.

1. Introduction

The quality of the semiconductor crystals grown from liquid melts is known to depend heavily on the buoyancy induced transport processes in the liquid melts particularly in the vicinity of the melt–crystal interface. The unsteady heat transfer rate in the growing interface resulting from the unstable temperature field, in the form of transient fluctuating temperature in the liquid melts, driven by the high buoyancy will cause striations in the crystal. In addition, the non-uniform heat transfer rate on the interface will result in a curved interface. Control of the thermal boundary conditions on the crucible containing the melt and use of the crucible rotation to produce a stable and uniform heat transfer rate at the interface are most desirable. Thus, crucibles are often rotated to suppress the thermal buoyancy induced velocity and temperature oscillation with time in the fluid phase and to obtain spatially uniform solidification or deposition rate of the solid phase. But the details on the complex flow fluctuation characteristics driven by the simultaneous presence of the thermal buoyancy and rotation induced Coriolis and centrifugal forces are still poorly understood. Hence, the effects of the crucible rotation on the thermally flow fluctuation need to be investigated. This study intends to explore how the interactions between the crucible rotation and thermal buoyancy affect the temperature fluctuation in liquid water contained in a crucible. The closed cylinder is chosen as the crucible since it is used in the growth of bulk crystals from the vertical Bridgman method [1]. In particular, we investigate how the cylinder rotation about its own axis affects the thermal characteristics of

* Corresponding author. Tel.: +886-35712121-55118; fax: +886-35726440.

E-mail address: u8614812@cc.nctu.edu.tw (T.F. Lin).

0017-9310/01/$ - see front matter
PII: S0017-9310(00)00146-0

Nomenclature

Ar	aspect ratio, H/D
D	diameter of right cylinder
f_1	main oscillation frequency
f_2	second oscillation frequency
H	height of cylinder
Pr	Prandtl number
PSD	power spectrum density
r, ϕ, z	dimensional coordinate systems of cylinder
R, Φ, Z	dimensionless coordinate systems of cylinder, r/D, ϕ, z/D
Ra	Rayleigh number, $\beta g \Delta T D^3/\alpha v$
Ra_{c1}	lower critical Rayleigh number
Ra_{c2}	upper critical Rayleigh number
Re_Ω	rotational Reynolds number, $\Omega D^2/v$
T	local temperature
Ta	Taylor number, $\Omega^2 D^4/v^2$
T_H	temperature of the hot wall
T_L	temperature of the cold wall

Greek symbols

α	thermal diffusivity
β	thermal expansion coefficient
ΔT	temperature difference between the hot and cold walls, $T_H - T_L$
θ	dimensionless temperature, $(T - T_L)/(T_H - T_L)$
θ_{av}	non-dimensional space and time-averaged temperature
$\overline{(\theta - \theta_{av})^2}$	non-dimensional space and time-averaged energy of temperature fluctuation
μ	dynamic viscosity
v	kinematic viscosity
ε	radiant emissivity
ρ	water density at temperature, T
τ	dimensionless time, $t/(D^2/\alpha)$
Ω	rotating rate

the buoyancy driven water flow in a bottom heated vertical cylinder by measuring time variations of the fluid temperature at various rotation rates.

Suitable models to approximate the buoyancy driven convection in various vertical melt growth configurations have been proposed by Müller et al. [1]. Meanwhile, a model experiment was conducted to visualize the water flow in a bottom heated cylinder of unit aspect ratio for various thermal conditions covering the steady and unsteady convection. Axisymmetric numerical simulation was carried out by Huang and Hsieh [2] and Lin and Akins [3,4] to investigate natural convection in a bottom heated vertical cylinder. Two different melts, water ($Pr = 6.7$) and gallium ($Pr = 0.02$), have been investigated for various aspect ratios and for the Rayleigh number up to 10^8. Both experimental results and numerical analysis for the onset of convection and the state of convection flow were presented by Müller et al. [5]. Similar analysis was performed by Neumann [6] for steady and oscillatory convection. The limits for the appearance of the stable axisymmetric flow were found. The onset of the transient flow oscillation and the induced oscillation frequency were also calculated. Three-dimensional steady flow was numerically simulated by Crespo and Bontoux [7] to investigate asymmetric steady flow motion in a liquid layer confined in a stationary vertical circular cylinder heated from below.

Visualization of the flow of a high Prandtl fluid (silicone oil with $Pr = 10^5$) in a stationary vertical cylinder revealed axisymmetric flow at a slightly supercritical Rayleigh number and two distinct three-dimensional flow motions at increasing Rayleigh number [8]. Various routes for the transition from steady laminar flow to the unsteady chaotic flow were determined according to the temperature fluctuation data by Rosenberger and his co-workers [9,10] for the Xenon gas in a bottom heated vertical cylinder. Similar experimental study was conducted by Kamotani et al. [11] for gallium ($Pr = 0.027$) for both vertical and inclined cylinders. Based on the transient temperature data measured on the lateral side of the cylinder they suggested various convection flow patterns. The non-axisymmetric convection in a vertical directional solidification experiment in a vertical cylinder was ascribed to the lack of azimuthal symmetry in the imposed temperature boundary condition by Pulicani et al. [12]. Modification of the interface shape to a flat profile from the use of appropriate temperature gradients in the vertical Bridgman growth was studied by Feigelson and Route [13]. Kirdyashkin and Distanov [14] found that a periodically changing rotation speed can result in periodic temperature change throughout the entire liquid layer. Rossby [15] examined the effects of rotation on the Bënard convection by considering a thin horizontal layer of fluid rotating about a vertical axis when it is subject to uniform heating from below and cooling from above. His study has led to more precise description of the stability properties of Bënard convection over a wide range of the Taylor numbers for water ($Pr = 6.8$) and mercury ($Pr = 0.025$). For water subject to the thermal Rayleigh number Ra ($= \beta g \Delta T D^3/\alpha v$) ranging from 10^6 to 2×10^{11} and Taylor number Ta ($= \Omega^2 D^4/v^2$) from 10^6 to 10^{12}, Boubnov and Golitsyn [16] observed a ring pattern of convection flow resulting from the fluid spin-up and vortex interactions between

two adjacent vortices. Axisymmetric secondary flow was noted by Guo and Zhang [17] in a vertically rotating cylinder heated from below even under zero gravity condition.

Centrifugal driven thermal convection in a vertical rotating cylinder heated from above has been considered by Homsy and Hudson [18]. They noted that the axial flow was strongly influenced by the horizontal Ekman layers and gravity is seen to have at most only a local effect on the flow near the side walls, whereas heat transfer was considerably increased by the cylinder rotation. In a further study [19], they conducted a mathematical analysis and revealed the effects of the side wall and heat losses on the Nusselt numbers on the top and bottom surfaces of the cylinder. Experiments for silicone oil carried out by Hudson and his coworkers [20,21] indicated that the Nusselt number increased with the rotation rate. Pfotenhauer and Niemela [22] reported that both the Rayleigh number associated with the convective onset and the convection heat transfer were found to depend on the rotation rate and aspect ratio of the cell for liquid helium. The onset of steady natural convection in the cylinder was shown by Buell and Catton [23] to be sensitive to lateral thermal boundary condition. Laminar natural convection in a fluid-filled cylinder with different end wall temperatures was investigated in a three-dimensional numerical study by Schneider and Straub [24]. The onset of convection in a low Prandtl number fluid confined in a rotating vertical cylinder heated from below was studied by Goldstein et al. [25]. The linear stability problem was solved for various boundary conditions.

The above literature review clearly indicates that the detailed flow structures driven simultaneously by the thermal buoyancy and rotation in a liquid-filled vertical cylinder remain largely unexplored and our understanding on the stabilization of the natural convection flow by the crucible rotation associated with the vertical Bridgman growth is still poor. Thus, the detailed processes on how the rotation affects the flow stability and the unsteady flow characteristics need to be investigated. Considering the difficulty in measuring and visualizing the rotating enclosed flow, comprehensive temperature measurements are carried out in the present study to unravel the effects of the cylinder rotation on the flow stabilization and to delineate the fluctuating characteristics of the unsteady flow in a bottom heated, rotating cylinder containing liquid water.

2. Experimental apparatus

The experimental system for measuring the thermal characteristics in a rotating vertical cylinder filled with distilled water schematically shown in Fig. 1 consists of four parts, namely, a rotating frame, a test section, a

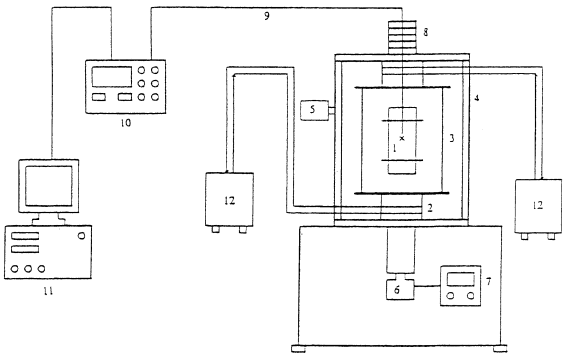

1: test section
2: fluid slip ring
3: rotating frame
4: static frame
5: photo-electric tachometer
6: Hp induction motor
7: invert
8: slip ring
9: thermocouples
10: data acquisition system
11: P.C. computer
12: thermostat

Fig. 1. Schematic diagram for the experimental system.

temperature control unit and a temperature measuring unit. Fig. 2 shows the details of the test section, a water-filled cylinder, in the rotating assembly. The cylindrical cavity is rotated at a constant angular speed about its own axis.

The rotating frame is made up of a rotary table of 31.5 cm in diameter and is mounted on a steel shaft of 3 cm in diameter. The frame is designed to provide a space of 27.6 cm in diameter and 27.3 cm in height for housing the test section. The shaft is rotated by a 2 horse power d.c. motor with its speed controlled by an inverter. Besides, the rotating speed is detected by a photoelectric tachometer. Care is taken to ensure that the table rotates centrally and steadily. Two fluid sliprings are used to allow coolants to pass from stationary thermostats to the rotating cavity. The thermostats used are LAUDA RK-20 compact constant temperature baths with a temperature range from −40°C to 150°C and a resolution of 0.1°C. Care must be taken to prevent coolant leak from the fluid sliprings and the distilled water leak from the rotation cylinder. Through this arrangement, the temperature uniformity of the isothermal plates can be controlled to within ±0.1°C.

For temperature measurement, thermocouple connections are carefully placed in the rotating cylinders. The thermocouples in the rotating cylinders are fixed at designated locations by high performance fine Neoflon threads, which are in turn fixed on the sidewall and passed through the axis of the cylinder. Prior to installation, the thermocouples are calibrated by the LAUDA thermostats and high precision liquid-in-glass thermometers. Voltage signals from the thermocouples are passed through a slipring to the HP 3852A data acquisition system and then transmitted to a personal

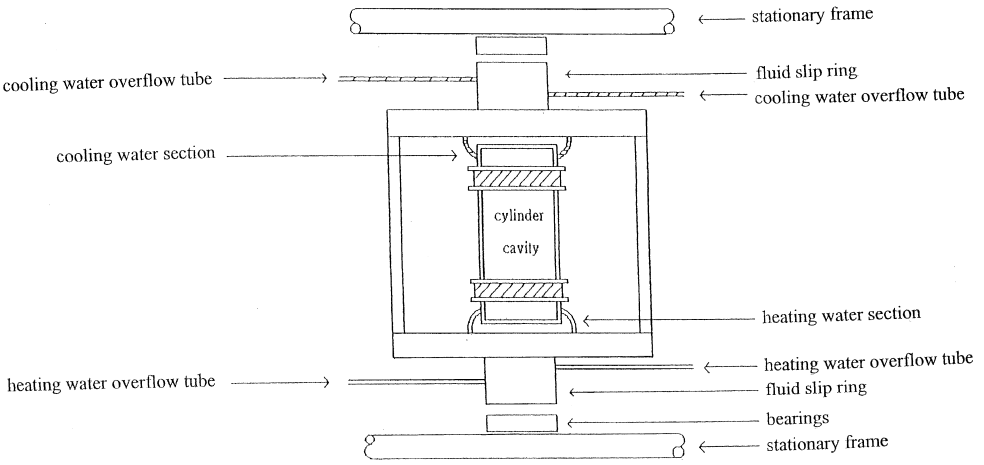

Fig. 2. Rotating assembly for vertical circular cylinder.

computer for further data processing. Data collection is normally started when the flow already reaches steady or statistically stable state. In view of the buoyancy driven low speed flow encountered in the rotating cavity, velocity measurement is difficult and is not conducted in the study.

The test section fixed on the rotating table is a water-filled circular cylinder of 5 cm in diameter and 10 cm in height or 2.5 cm in diameter and 5 cm in height. The sidewalls of the cylinders are made of 5 mm thick acrylic plates. In order to reduce heat loss from the sidewall, the cylinder was wrapped with superlon foam. The top and bottom of each cylinder are made of two 2 mm thick copper plates with 8 mm thick MEGABOND OB-101 epoxy sandwiched between them (Fig. 3). The hot and cold walls of the cylinders consist of well-polished copper plates with a small radiant emissivity ε ($=0.06$). Their temperatures are controlled at the designated levels by passing coolants from the constant temperature baths through the plates and monitored by the imbedded thermocouples. The sampled measured data for the temperature of the hot and cold isothermal walls without rotation at selected locations are given in Table 1 for the large cylinder with $H=10$ cm and $D=5$ cm and for the small cylinder with $H=5$ cm and $D=2.5$ cm.

Test was started by first setting the thermostats at predetermined temperatures and then recirculating the coolants through the two designated isothermal walls of the rotating cylinder. The average value of the hot and cold plate temperatures is adjusted to be approximately equal to the ambient temperature so that heat loss from the test section to the ambient can be reduced and thermal radiation across the plates is minimized. In the meantime, the cylinder was rotated at the predetermined speed. Then, the temperature of the water inside the cavity was measured at selected locations. In addition, it is very essential to insure that the time-average variation

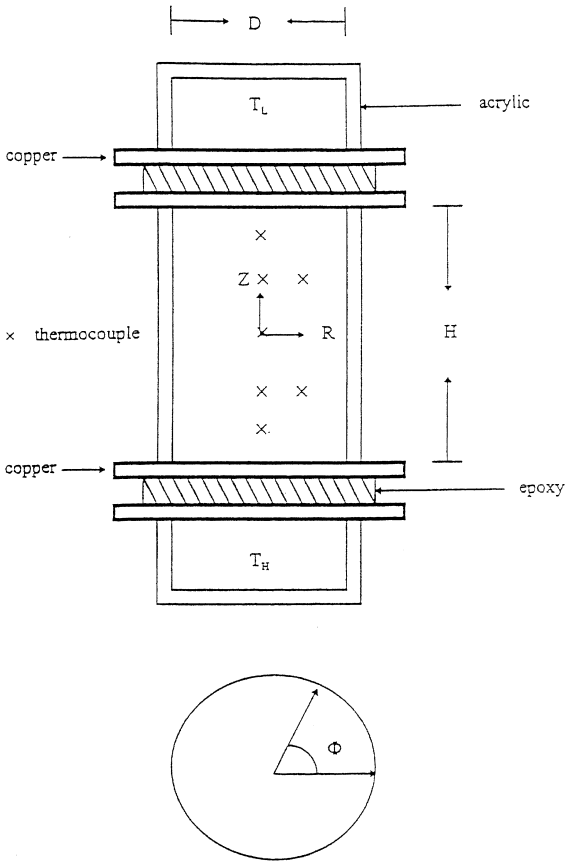

Fig. 3. The coordinate system and the locations of thermocouples for circular cylinder with $D=5$ cm and $H=10$ cm.

of the signal from each thermocouple is below 0.1°C for a period of at least 15 min and at this steady or statistically stable state data collection is started. The period of time required for the flow to reach the steady or

Table 1
Temperature uniformity in isothermal walls for $\Omega = 0$ of circular cylinder with (a) $D = 5$ cm and $H = 10$ cm and (b) $D = 2.5$ cm and $H = 5$ cm

Location (R, Φ)	T_L (°C)	T_H (°C)
(a)		
$(0, 0)$	29.36	35.87
$(0.25, 0)$	29.27	35.72
$(0.25, 0.5\pi)$	29.30	35.74
$(0.25, \pi)$	29.26	35.77
$(0.25, 1.5\pi)$	29.23	35.85
$(0.5, 0)$	29.23	35.76
$(0.5, 0.5\pi)$	29.25	35.74
$(0.5, \pi)$	29.28	35.79
$(0.5, 1.5\pi)$	29.32	35.75
(b)		
$(0, 0)$	15.09	25.22
$(0.25, 0)$	15.01	25.24
$(0.25, 0.5\pi)$	14.97	25.19
$(0.25, \pi)$	15.05	25.28
$(0.25, 1.5\pi)$	15.03	25.17
$(0.5, 0)$	14.99	25.30
$(0.5, 0.5\pi)$	15.06	25.24
$(0.5, \pi)$	15.08	25.27
$(0.5, 1.5\pi)$	14.95	25.20

statistically stable state condition in the present experiment is about $0.3D^2/\alpha$.

The ranges of the governing parameters to be investigated in the study are as follows: the rotating speed varied from 0 to 300 rpm for the large cylinder with $D = 5$ cm and from 0 to 210 rpm for the small cylinder with $D = 2.5$ cm. The top and bottom wall temperature difference ΔT is fixed at 5°C, 10°C or 15°C. The results from an uncertainty analysis of the measurement are summarized in Table 2. Before the actual data collection, we tested the background noise of the experimental apparatus with $\Delta T = 0$°C in the cylinder and varying the rotating speed from 0 to 120 rpm. Results indicated that the amplitude of the temperature oscillation is less than ±0.1°C, and hence we can define that the water flow in the cylinder is steady when the temperature oscillation is in the order of ±0.1°C.

Table 2
Summary of uncertainty analysis for cylinders

Parameters	Uncertainty
D (m)	±0.00025
H (m)	±0.00025
T_H, T_L (°C)	±0.1 (non-rotating)
T_H, T_L (°C)	±0.2 (rotating)
T (thermcouple)	±0.5°C
α (m^2/s)	±0.01%
β (K^{-1})	±0.05%
ρ (kg/m^3)	±0.001%
k (mW/m K)	±0.01%
μ (μPa s)	±0.1%
ν (m^2/s)	±0.07%
Ω (rpm)	±0.3%
Pr	±0.1%
Ra	±2.05%
Ra_Ω	±4.3%
Re_Ω	±2.025%

3. Results and discussion

There are two cylinders tested in the present study with $D = 2.5$ and 5 cm at the same aspect ratio $Ar = 2$, as mentioned above. Attention is mainly focused on the axial distributions of the time-average temperature and the change in the amplitude and frequency of the instantaneous temperature oscillation with the rotation rates at different imposed temperature differences.

3.1. Effects of rotation on time-average temperature

The dimensionless time-average water temperature variations with the axial coordinate $Z(= z/D)$ along the cylinder axis were measured first at different rotation rates Ω and temperature differences ΔT. The coordinate system is chosen to rotate with the cavity with its origin located at the geometric center of the cavity, as indicated in Fig. 3. The locations of the thermocouples are also indicated in the figure. Typical data from this test for the large cylinder with $D = 5$ cm are exemplified in Fig. 4 for $\Delta T = 5$°C at increasing Ω. The corresponding thermal Rayleigh number Ra for these cases is 1.02×10^7. It is noted from these data that in a non-rotating cylinder ($\Omega = 0$) large vertical temperature gradients exist in the regions near the top and bottom of the cavity due to the presence of thermal boundary layers there (Fig. 4). Outside these thermal boundary layers in the cavity core the flow is nearly isothermal. Similar situation is noted at low rotating rates of $\Omega = 20$, 40, 60 rpm. This unique temperature distribution at a low Ω is considered to result from the dominated thermal buoyancy driven boundary layer flow in the cylinder at this high thermal Rayleigh number. As the cylinder rotates at higher speeds of 90 and 120 rpm, the temperature gradients near the horizontal plates are significantly reduced and in the cylinder core the temperature varies almost linearly in the vertical direction. This trend continues as the rotation rate is further raised. For $\Omega \geqslant 180$ rpm almost no thermal boundary layer exists in the cavity and the water temperature varies nearly linearly from the hot bottom plate to the cold top plate. This conduction-like temperature distribution is conjectured to result from the suppression of the thermal buoyancy driven flow by the Coriolis force associated with the cavity rotation, as noted in a previous numerical simulation for convection in a rotating cubic air cavity by Lee and Lin [26]. Similar

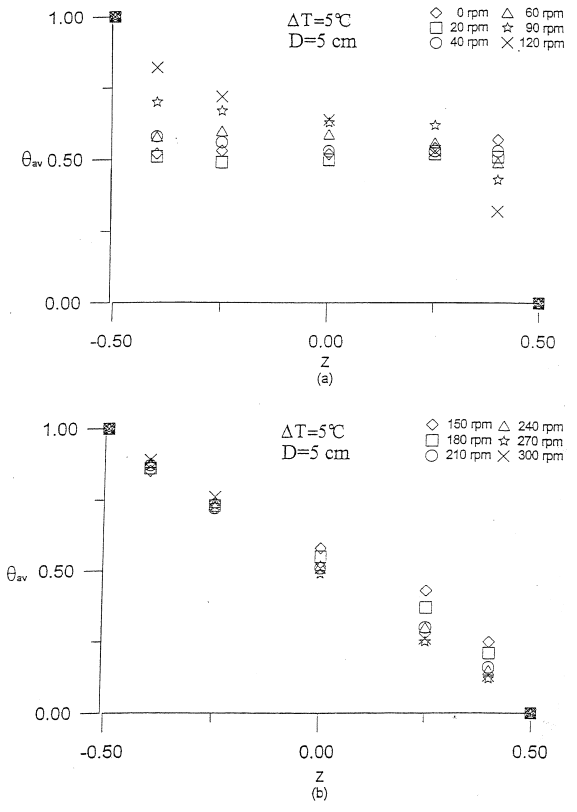

Fig. 4. Non-dimensional time-average temperature distribution along Z-axis for a vertical circular cylinder with $D=5$ cm and $H=10$ cm at $\Delta T=5°C$ ($Ra=1.02\times10^7$) for different rotation rates for (a) 0–120 rpm and (b) 150–300 rpm.

trend was noted for $\Delta T=10°C$ and 15°C. It is also noted that for a larger temperature difference ΔT across the horizontal plates a higher rotation rate is required to suppress the thermal buoyancy driven flow. Similar trend was found for the axial variation of the time-average temperature in the small cylinder with $D=2.5$ cm.

3.2. Rotation induced flow stabilization

The rotation induced flow transition among the steady and time dependent states in the bottom heated cylinder is then investigated by examining the time variations of the measured instantaneous water temperature at selected locations in the cavity. Only the long time results are studied at which the temperature already reaches steady or statistically stable state.

The temporal stability of the water flow affected by the cylinder rotation is illustrated by the measured temperature data at location $(R,\Phi,Z)=(0,0,0)$ for $\Delta T=5°C$ ($Ra=1.02\times10^7$) shown in Fig. 5 for the large cylinder. Since only the data at the statistically stable state are recorded, the dimensionless time $\tau(t/(D^2/\alpha))=0$ stands for a certain arbitrary time instant at that state. The results at various rotation rates manifest that at $\Omega=0$ the flow oscillates chaotically in time with the amplitude of the temperature oscillation being larger than 0.1 in a dimensionless unit or larger than 0.5°C dimensionally. At slightly higher Ω of 20 and 40 rpm the flow also oscillates irregularly but in slightly larger amplitude and slower pace. For a rise of Ω to 60 rpm, the temperature oscillation is significantly reduced. But the flow is not completely stabilized. A small increase of Ω to 90 rpm causes the flow to oscillate periodically in time. Note that at $\Omega=90$ rpm the oscillation amplitude is all below 0.025 in a dimensionless temperature unit or less than 0.15°C dimensionally. This amplitude of the oscillation is of the same order as the background noise always existing in the test apparatus and the flow can be regarded as steady. Thus, the flow experiences a reverse Hopf bifurcation, a transition from a periodic to a steady state. A further raise of Ω to 120, 150 and 180 rpm results in even lower oscillation amplitudes. Obviously, the flow can be considered as steady. As Ω is raised over 210 rpm the oscillation amplitude grows noticeably with the rotation rate. Specifically, at $\Omega=210$ rpm the oscillation amplitude is 0.25°C and the temperature oscillation is intermittent with the high frequency wave packets superimposed on a low frequency small amplitude cycle. For higher Ω of 240, 270 and 300 rpm, the flow is in large amplitude periodic or quasi-periodic oscillation. The above results for $\Delta T=5°C$ at various Ω clearly suggest that the cavity rotation introduces a non-monotonic change in the oscillation amplitude at increasing rotation rate. More importantly, a finite range of rotation rate exists for the axial cylinder rotation to effectively stabilize the thermal buoyancy driven unstable water flow.

When the large cylinder is subject to a much larger temperature difference of $\Delta T=10°C$ ($Ra=2.04\times10^7$) the thermal buoyancy is so high that the induced flow is in a large amplitude chaotic oscillation when the cylinder is non-rotating. Increases of Ω from 0 to 20, 40, 60, and 90 rpm do not stabilize the flow to any noticeable degree. At a slightly higher Ω of 120 rpm the flow is in fact steady at the location $(0,0,0)$. It is of interest to note from the data for other detection points that the flow is in a small amplitude oscillation only at the location $(0,0,0)$ for $\Omega=120$ rpm. In fact, the flow was chaotic at the other locations. The spatial dependence of the flow oscillation will be examined later. Substantial reduction in the oscillation amplitude occurs when Ω is raised to 150, 165 and 180 rpm. The oscillation amplitudes are all about 0.018 dimensionlessly or 0.18°C dimensionally, which is of the same order as the background disturbances. Hence, the flow can be regarded as steady. This clearly shows the flow stabilization by the cavity rotation when the rotation rate ranges from 150 to 180 rpm. At an even higher Ω of 210 rpm or over, the flow os-

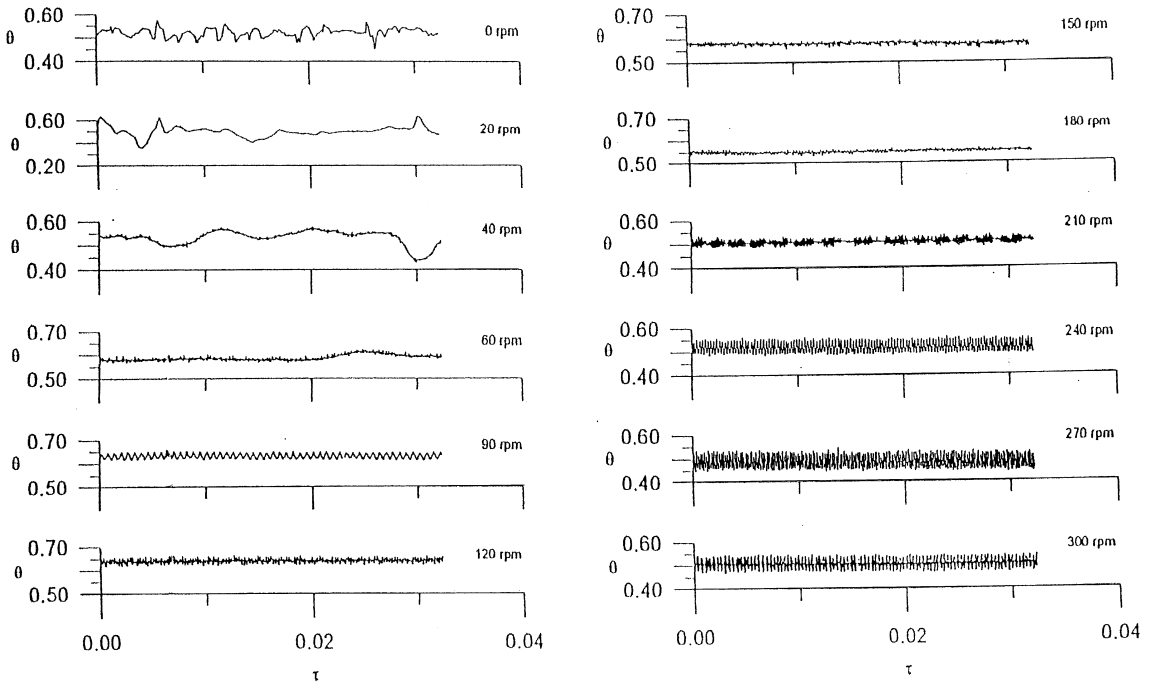

Fig. 5. Measured time records of water temperature for vertical circular cylinder with $D=5$ cm and $H=10$ cm at location $(R, \Phi, Z)=(0, 0, 0)$ for various rotation rates at $\Delta T=5°C$ ($Ra=1.02\times10^7$).

cillates periodically or quasi-periodically in a noticeable degree as that for $\Delta T=5°C$. Similar trend can be found for the rotation induced flow stability for a higher thermal buoyancy at $\Delta T=15°C$ ($Ra=3.06\times10^7$). The results suggest that for Ω ranging from 0 to 90 rpm the flow is in chaotic oscillation. The thermal buoyancy here is so high that the induced flow oscillation is stronger than those for $\Delta T=5°C$ and 10°C as the cavity is at a low rotation rate. But at $\Omega=120$, 150 and 180 rpm, the temperature oscillation is rather small and the flow is steady at the location (0, 0, 0).

The temporal stability of the water flow in the small cylinder is somewhat different. The measured data for $\Delta T=5°C$ ($Ra=1.28\times10^6$) indicated that at $\Omega=0$ rpm the flow is in a very small amplitude oscillation and can be regarded as steady. Similar flow condition was found at $\Omega=20$ rpm. As the cylinder was rotated at 40 rpm, the flow was in a larger amplitude, low frequency time periodic oscillation ($f_1=0.0018$). Thus, the flow experienced a Hopf bifurcation, a transition from a steady to a time periodic state, for a raise of Ω from 20 to 40 rpm. A small increase of Ω to 60 rpm caused the flow to oscillate in an even smaller frequency but still in higher amplitude. It was of interest to note that for further increases of Ω to 90 and 120 rpm the flow was stabilized and became steady. Therefore, a reverse Hopf bifurcation occurred for Ω raising from 60 to 90 rpm. At a higher Ω of 150 rpm the flow exhibited a discernible low frequency high amplitude oscillation with a very small amplitude high frequency oscillation superimposed on it. At slightly higher rotation rates of 180 and 210 rpm the high frequency component grew slightly in amplitude.

When the small cylinder is subject to a much larger temperature difference of $\Delta T=10°C$ ($Ra=2.55\times10^6$) the thermal buoyancy is so high that the induced flow is in a large amplitude chaotic oscillation as the cavity is stationary ($\Omega=0$), as clear from the data in Fig. 6. At slightly higher rotation rates of 20 and 40 rpm the chaotic flow is in a larger amplitude oscillation. Note that the flow becomes time periodic and oscillates slowly but in larger amplitude when the cylinder rotates at 60 rpm ($f_1=0.0013$). Substantial reduction in the oscillation amplitude occurs when Ω is raised to 90, 120 and 150 rpm. More specifically, the oscillation amplitude is less than 0.2°C dimensionally, which is of the same order as the background disturbances. Hence, the flow can be regarded as steady. This clearly shows the flow stabilization by the cavity rotation when the rotation rate ranges from 90 to 150 rpm. When the rotation rate continues to increase from 150 to 180 and 210 rpm, the flow undergoes a transition from a steady to a time periodic state. The flow is dominated by a low frequency high amplitude oscillation. Similar trend can be found for the effects of the cylinder rotation on the flow stability for a higher thermal buoyancy at $\Delta T=15°C$ ($Ra=3.83\times10^6$). For $\Delta T=15°C$, the stronger thermal

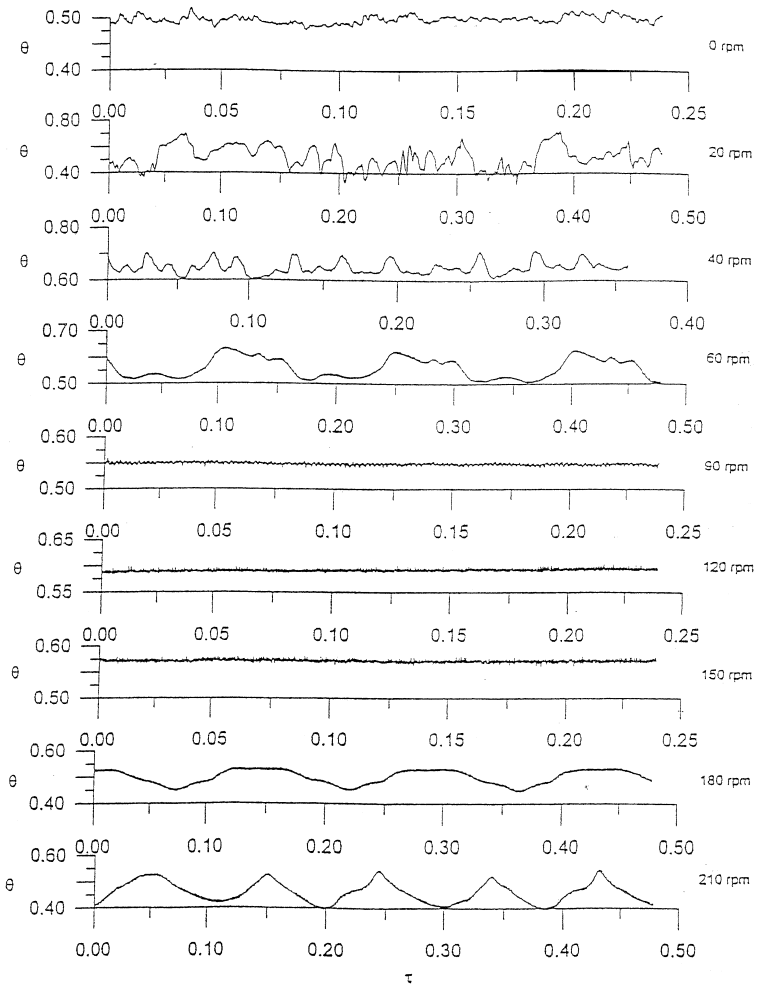

Fig. 6. Measured time records of water temperature for vertical circular cylinder with $D=2.5$ cm and $H=5$ cm at location $(R, \Phi, Z)=(0.25, 0, 0.25)$ for various rotation rates at $\Delta T=10°C$ ($Ra=2.55\times10^6$).

buoyancy induced flow is in a larger amplitude chaotic oscillation at $\Omega=0$ and 20 rpm. At a higher Ω of 40 rpm the flow exhibits a time periodic, high frequency oscillation. However, a large reduction in the oscillation frequency ensues for a rise of Ω to 60 and 90 rpm but the oscillation amplitude is larger. The oscillation amplitude decays significantly but the oscillation frequency increases substantially for a small rise of Ω to 120 rpm. As Ω is at 150 and 180 rpm the flow is in fact steady. As the cylinder is rotated at 210 rpm the flow experiences a transition from a steady to a time periodic state.

The spatial dependence of the temperature oscillation is examined next. Typical data to illustrate this dependence are shown in Fig. 7 by displaying the time histories of the water temperature at six selected locations in the large cylinder at $\Omega=165$ and 270 rpm for $\Delta T=10°C$. These results clearly show that substantial change in the oscillation amplitude with the location does exist. Note that at $\Omega=165$ rpm the oscillation amplitude is the smallest at the geometric center of the cylinder when compared with those at the other selected locations. But the reverse is the case for $\Omega=270$ rpm. In spite of the large spatial change in the oscillation amplitude, the flow at all the detected locations oscillates at nearly the same frequency when the flow is time periodic. The data for the small cylinder resemble those for the large cylinder discussed above.

3.3. Frequency content of flow oscillation

To further illustrate the characteristics of the flow oscillation, the power spectrum densities (PSDs) of the measured time histories for the time periodic and quasi-periodic cases were obtained by a fast Fourier transform analysis. The results from this analysis shown in Fig. 8 for $\Delta T=5°C$, 10°C and 15°C at location $(R, \Phi, Z)=$

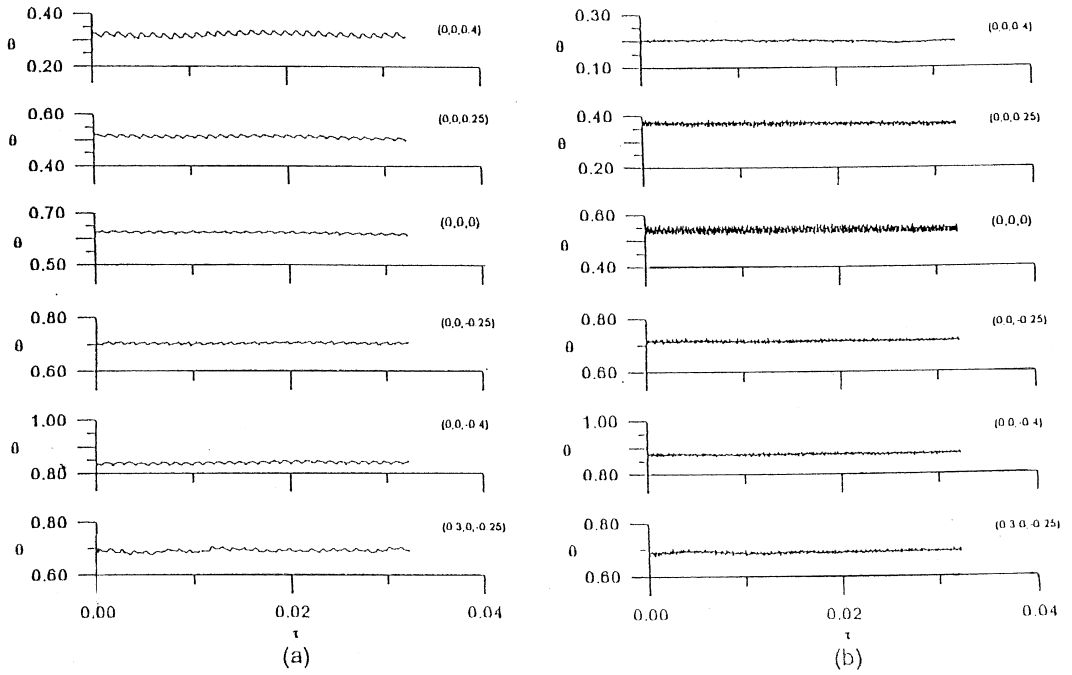

Fig. 7. Measured time histories of water temperature at various locations for $\Delta T = 10°C$ ($Ra = 2.04 \times 10^7$) for (a) $\Omega = 165$ rpm ($Re_\Omega = 4.49 \times 10^4$) and (b) $\Omega = 270$ rpm ($Re_\Omega = 7.34 \times 10^4$) for vertical circular cylinder with $D = 5$ cm and $H = 10$ cm.

(0, 0, 0) in the large cylinder for various rotation rates indicate that the effects of the thermal buoyancy (temperature difference) on the oscillation frequency are small, as evident from the comparison of the corresponding plots at the same Ω for different ΔT. However, the change in the oscillation amplitude (the value of PSD) with the temperature difference and rotation rate is noticeable. Examining the results in Fig. 8(a) for $\Delta T = 5°C$ discloses that at $\Omega = 180$ rpm a distinct frequency peak exists. For a slightly higher Ω of 210 rpm the oscillation frequency is much higher. However, a large drop in the oscillation frequency ensues for a rise of Ω to 240 rpm, followed by an increase in the frequency for further rises of Ω to 270 and 300 rpm. Furthermore, a close inspection of the plots in Fig. 8(a) reveals that another frequency peak also exists in each plot, which is rather low and coincides almost with the vertical axis. Thus, the flow is actually quasi-periodic. The above results from the PSD analysis clearly indicate that in the rotating cylinder the temperature oscillation is mainly dominated by a single frequency when the flow is time periodic or quasi-periodic. Similar characteristics in the change of the dominant oscillation frequency with the rotation rate for higher ΔT are noted in Figs. 8(b) and (c). Sampled results of the main oscillation frequency f_1 for the time periodic cases and the first and second fundamental frequencies f_1 and f_2 for the quasi-periodic cases along with the flow condition at statistical state are given in Table 3 for the large and small cylinders.

It is of interest to compare the above data for water in the rotating cylinder with those for air in our previous study [27] for $D = 5$ cm. Based on the thermal diffusion time D^2/α for water and air, the non-dimensional oscillation frequency in the water cavity is much higher than that in the air.

3.4. Energy of temperature oscillation

An overall characteristic of the flow stabilization by the axial cylinder rotation can be conveniently expressed by the temporal–spatial average energy of the dimensionless water temperature fluctuation $\overline{(\theta - \theta_{av})^2}$. The quantity θ_{av} is based on the simultaneous average of the instantaneous temperature in time and in all detected locations. Typical results for the average energy of the temperature fluctuation in the large cylinder at various rotation rates are shown in Fig. 9 for $\Delta T = 5°C$, 10°C and 15°C. The effects of the cavity rotation on the flow stability can be clearly seen from these results. In the range of the stable region the fluctuation energy is small. Similar results were obtained for the small cylinder.

3.5. Correlations for stable regions

Based on the data from the present investigation for the two cylinders, the critical Rayleigh numbers Ra_{c1} and Ra_{c2} for the existence of the main stable flow region

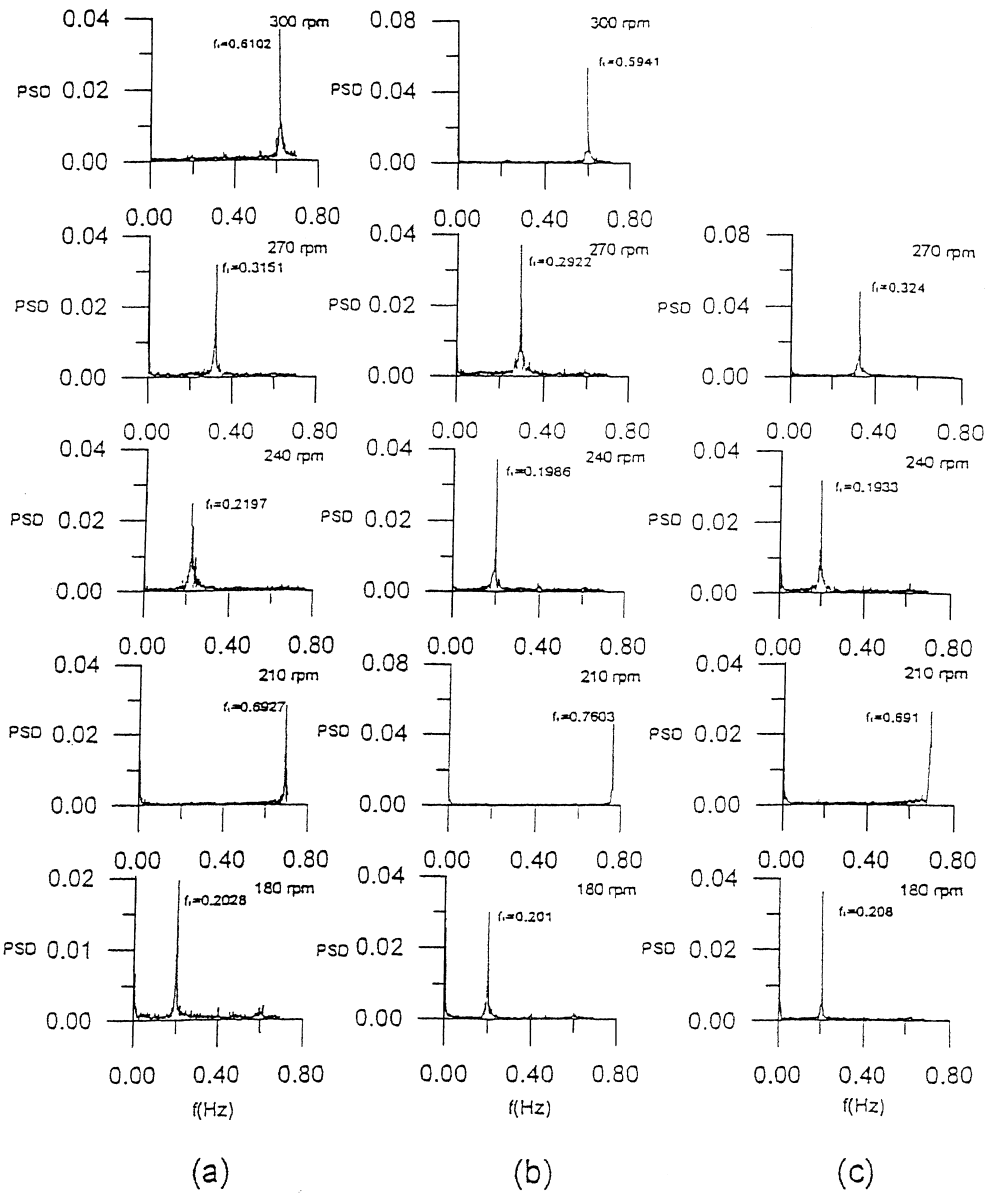

Fig. 8. PSDs of water temperature for vertical circular cylinder with $D=5$ cm and $H=10$ cm at location $(R, \Phi, Z)=(0, 0, 0)$ for various rotation rates at (a) $\Delta T=5$°C ($Ra=1.02\times10^7$), (b) $\Delta T=10$°C ($Ra=2.04\times10^7$) and (c) $\Delta T=15$°C ($Ra=3.06\times10^7$).

in the cylinders can be correlated with the rotation Reynolds number Re_Ω ($Re_\Omega=\Omega D^2/\nu$).

The lower critical Rayleigh number Ra_{c1}

$$\log Ra_{c1}=5.34+1.52\times10^{-1}(Re_\Omega)-4.92\times10^{-3}(Re_\Omega)^2+5.38\times10^{-5}(Re_\Omega)^3,$$
$$6\leqslant(Re_\Omega\times10^{-3})\leqslant50.$$

The upper critical Rayleigh number Ra_{c2}

$$\log Ra_{c2}=6.21+3.596\times10^{-3}(Re_\Omega)-1.135\times10^{-4}(Re_\Omega)^2,$$
$$6\leqslant(Re_\Omega\times10^{-3})\leqslant40.$$

Fig. 10 compares the above correlations with the present data.

4. Concluding remarks

The fluctuating characteristics of the buoyancy driven unstable water flow in closed cylinders affected by the axial cylinder rotation were investigated experimentally by transient temperature measurement in the present study. The results were obtained for the thermal Rayleigh number ranging from 1.02×10^7 to 3.06×10^7

Table 3
Summary of flow characteristics for cylinders with (a) $D=5$ cm and $H=10$ cm and (b) $D=2.5$ cm and $H=5$ cm

Rotation rate (rpm)	$\Delta T=5$°C			$\Delta T=10$°C			$\Delta T=15$°C		
	Flow condition	f_1	f_2	Flow condition	f_1	f_2	Flow condition	f_1	f_2
(a)									
0	Chaotic	–	–	Chaotic	–	–	Chaotic	–	–
20	Chaotic	–	–	Chaotic	–	–	Chaotic	–	–
40	Chaotic	–	–	Chaotic	–	–	Chaotic	–	–
60	Chaotic	–	–	Chaotic	–	–	Chaotic	–	–
90	Steady	–	–	Chaotic	–	–	Chaotic	–	–
120	Steady	–	–	Chaotic	–	–	Chaotic	–	–
150	Steady	–	–	Steady	–	–	Steady	–	–
165	–	–	–	Steady	–	–	–	–	–
180	Periodic	0.2028	–	Steady	–	–	Periodic	0.208	–
210	Periodic	0.6927	–	Periodic	0.7603	–	Periodic	0.691	–
240	Periodic	0.2197	–	Periodic	0.1986	–	Periodic	0.1933	–
270	Periodic	0.3151	–	Periodic	0.2922	–	Periodic	0.324	–
300	Periodic	0.6102	–	Periodic	0.5941	–	–	–	–
(b)									
0	Steady	–	–	Chaotic	–	–	Chaotic	–	–
20	Steady	–	–	Chaotic	–	–	Chaotic	–	–
40	Periodic	0.0018	–	Chaotic	–	–	Periodic	0.0436	0.083
60	Periodic	0.0009	–	Periodic	0.0013	–	Periodic	0.0013	–
90	Steady	–	–	Steady	–	–	Periodic	0.0021	–
120	Steady	–	–	Steady	–	–	Periodic	0.0106	–
150	Periodic	0.001	0.308	Steady	–	–	Steady	–	–
180	Periodic	0.0012	0.198	Periodic	0.0014	0.203	Steady	–	–
210	Periodic	0.0006	0.695	Periodic	0.0011	0.748	Periodic	0.0022	0.748

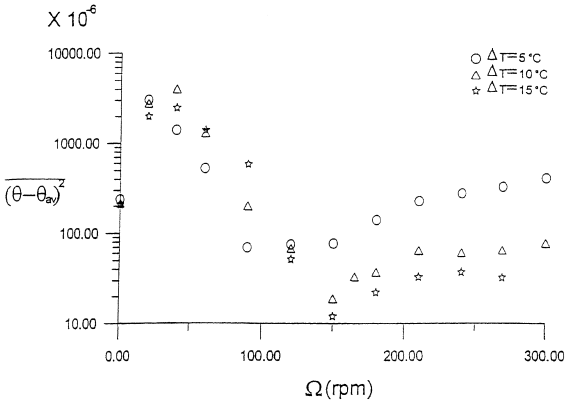

Fig. 9. The average energy of non-dimensional fluctuating temperature for the large vertical circular cylinder with $D=5$ cm and $H=10$ cm for various rotation rates and temperature differences.

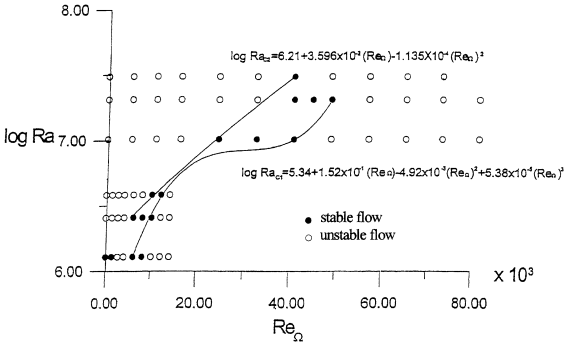

Fig. 10. Flow regime map and correlations for upper and lower critical Rayleigh numbers for stable flow region.

and rotational Reynolds number from 0 to 8.16×10^4 for the cylinder with $D=5$ cm and the thermal Rayleigh number from 1.28×10^6 to 3.83×10^6 and rotational Reynolds number from 0 to 1.43×10^4 for another cylinder with $D=2.5$ cm for $\mathrm{Ar}=2$. The major conclusions from this study suggest that the flow suppression by the cylinder rotation causes the time-average temperature distributions along the cylinder axis for high rotation rates to become linear. In addition, a finite range of the rotation rate exists for the thermal buoyancy driven unstable water flow to be stabilized. In spite of the large change in the oscillation amplitude in the space, the flow at all detected locations oscillates at almost the same frequency for the time periodic cases. The corresponding temperature oscillation is mainly dominated by a single fundamental frequency for each case. Besides, the

variation of the dominant frequency with the rotation rate is non-monotonic.

Acknowledgements

The financial support of this study by the engineering division of National Science Council of Taiwan, Republic of China through the contract NSC 83-0401 E-009-009 is greatly appreciated.

References

[1] G. Müller, G. Neumann, H. Matz, A two-Rayleigh-number model of buoyancy-driven convection in vertical melt growth configurations, J. Cryst. Growth 84 (1987) 36–49.
[2] D.Y. Huang, S.S. Hsieh, Analysis of natural convection in a cylinder enclosure, Numer. Heat Transfer 12 (1987) 121–135.
[3] Y.S. Lin, R.G. Akins, Pseudo-steady-state natural convection heat transfer inside a vertical cylinder, ASME J. Heat Transfer 108 (1986) 310–316.
[4] Y.S. Lin, R.G. Akins, Thermal description of pseudo steady state natural convection inside a vertical cylinder, Int. J. Heat Mass Transfer 29 (1986) 301–307.
[5] G. Müller, G. Neumann, W. Weber, Natural convection in vertical Bridgman configurations, J. Cryst. Growth 70 (1984) 78–93.
[6] G. Neumann, Three-dimensional numerical simulation of buoyancy-driven convection in vertical cylinders heated from below, J. Fluid Mech. 214 (1990) 559–578.
[7] E. Crespo Del Arco, P. Bontoux, Numerical solution and analysis of asymmetric convection in a vertical cylinder: an effect of Prandtl number, Phys. Fluids A 1 (1989) 1348–1359.
[8] R.S. Figliola, Convection transitions within a vertical cylinder heated from below, Phys. Fluids 29 (1986) 2028–2031.
[9] J.M. Olson, F. Rosenberger, Convective instabilities in a closed vertical cylinder heated from below. Part 1. Monocomponent gases, J. Fluid Mech. 92 (1978a) 609–629.
[10] J.R. Abernathey, F. Rosenberger, Time-dependent convective instabilities in a closed vertical cylinder heated from below, J. Fluid Mech. 160 (1985) 137–154.
[11] Y. Kamotani, F.B. Weng, S. Ostrach, Oscillatory natural convection of a liquid metal in circular cylinders, ASME J. Heat Transfer 1 (16) (1994) 627–632.
[12] J.P. Pulicani, S. Krukowski, J. Iwan, D. Alexander, J. Ouazzani, F. Rosenberger, Convection in an asymmetrically heated cylinder, Int. J. Heat Mass Transfer 35 (1992) 2119–2130.
[13] R.S. Feigelson, R.K. Route, Vertical Bridgman growth of CdGeAs2 with control of interface shape and orientation, J. Cryst. Growth 49 (1980) 261–273.
[14] A.G. Kirdyashkin, V.E. Distanov, Hydrodynamics and heat transfer in a vertical cylinder exposed to periodically varying centrifugal forces (accelerated crucible rotation technique), Int. J. Heat Mass Transfer 33 (1990) 1397–1415.
[15] H.T. Rossby, A study of Bënard convection with and without rotation, J. Fluid Mech. 36 (1969) 309–335.
[16] B.M. Boubnov, G.S. Golistyn, Experimental study of convective structures in rotating fluids, J. Fluid Mech. 167 (1986) 503–531.
[17] Z.Y. Guo, G.M. Zhang, Thermal drive in centrifugal fields mixed convection in a vertical rotating cylinder, Int. J. Heat Mass Transfer 35 (1992) 1635–1644.
[18] G.M. Homsy, J.L. Hudson, Centrifugally driven thermal convection in a rotating cylinder, J. Fluid Mech. 35 (1969) 33–52.
[19] G.M. Homsy, J.L. Hudson, Heat transfer in a rotating cylinder of fluid heated from above, Int. J. Heat Mass Transfer 14 (1971) 1149–1159.
[20] J.L. Hudson, D. Tang, S. Abell, Experiments on centrifugally driven thermal convection in a rotating cylinder, J. Fluid Mech. 86 (1978) 147–159.
[21] D. Tang, J.L. Hudson, Experiments on a rotating fluid heated from below, Int. J. Heat Mass Transfer 26 (1983) 943–949.
[22] J.M. Pfotenhauer, J.J. Niemela, Stability and heat transfer of rotating cryogen. Part 3. Effects of finite cylindrical geometry and rotation on the onset of convection, J. Fluid Mech. 175 (1987) 85–96.
[23] J.C. Buell, I. Catton, Effect of rotation on the stability of a bounded cylindrical layer of fluid heated from below, Phys. Fluids 26 (1982) 892–896.
[24] S. Schneider, J. Straub, Laminar natural convection in a cylindrical enclosure with different end temperatures, Int. J. Heat Mass Transfer 35 (1990) 545–557.
[25] H.F. Goldstein, E. Knobloch, I. Mercoder, M. Net, Convection in a rotating cylinder. Part 2. Linear theory for low Prandtl numbers, J. Fluid Mech. 262 (1993) 293–324.
[26] T.L. Lee, T.F. Lin, Transient three-dimensional convection of air in a differentially heated rotating cubic cavity, Int. J. Heat Mass Transfer 39 (1996) 1243–1255.
[27] Y.T. Ker, Y.H. Li, T.F. Lin, Experimental study of unsteady thermal characteristics and rotation induced stabilization of air convection in a bottom heated rotating vertical cylinder, Int. J. Heat Mass Transfer 41 (1998) 1445–1458.